Constraining the high-density nuclear symmetry energy with the transverse-momentum-dependent elliptic flow

Yongjia Wang,[1,2] Chenchen Guo,[1,3] Qingfeng Li,[1,*] Hongfei Zhang,[2] Y. Leifels,[4] and W. Trautmann[4]
[1]*School of Science, Huzhou Teachers College, Huzhou 313000, China*
[2]*School of Nuclear Science and Technology, Lanzhou University, Lanzhou 730000, China*
[3]*College of Nuclear Science and Technology, Beijing Normal University, Beijing 100875, China*
[4]*GSI Helmholtzzentrum für Schwerionenforschung GmbH, D-64291 Darmstadt, Germany*
(Received 10 February 2014; published 3 April 2014)

Within the newly updated version of the ultrarelativistic quantum molecular dynamics (UrQMD) model, the transverse-velocity dependence of the elliptic flow of free nucleons from ^{197}Au+^{197}Au collisions at the incident energy 400 MeV/nucleon is studied within different windows of the normalized c.m. rapidity y_0. It is found that the elliptic flow difference $v_2^n - v_2^p$ and ratio v_2^n/v_2^p of neutrons versus protons are sensitive to the density dependence of the symmetry energy, especially the ratio v_2^n/v_2^p at small transverse velocity in the intermediate rapidity intervals $0.4 < |y_0| < 0.6$. By comparing either transverse-momentum-dependent or integrated FOPI/LAND elliptic flow data of nucleons and hydrogen isotopes with calculations using various Skyrme interactions, all exhibiting similar values of isoscalar incompressibility but very different density dependences of the symmetry energy, a moderately soft to linear symmetry energy is extracted, in good agreement with previous UrQMD or Tübingen QMD model calculations but contrast with results obtained with π^-/π^+ yield ratios in the literature.

DOI: 10.1103/PhysRevC.89.044603 PACS number(s): 21.65.Cd, 21.65.Mn, 25.70.−z

I. INTRODUCTION

The nuclear symmetry energy, which plays an important role in studying exotic nuclei, heavy-ion collisions (HICs) with and without radioactive beams, and neutron stars, is a very active field of research in nuclear and astronuclear physics. It can be calculated from the parabolic approximation of the equation of state (EoS) of isospin asymmetric nuclear matter, $e(\rho,\delta) = e_0(\rho,0) + e_{\rm sym}(\rho)\delta^2$, where $\delta = (\rho_n - \rho_p)/(\rho_n + \rho_p)$ is the isospin asymmetry defined through the neutron (ρ_n) and proton (ρ_p) densities. The first term $e_0(\rho,0)$ is the energy per nucleon of isospin-symmetric nuclear matter which, at the saturation density ρ_0, is known as the binding energy E_0 of nuclear matter; the coefficient $e_{\rm sym}(\rho)$ of the second term is the bulk symmetry energy. There exists a large number of theoretical predictions for the density dependence of $e_{\rm sym}$ obtained with different many-body, effective-field, or phenomenological approaches. For a recent review, see Ref. [1].

Many practical attempts have been made to estimate parameters of the symmetry energy around saturation. They include the symmetry energy coefficient $S_0 = e_{\rm sym}(\rho_0)$, the slope parameter $L = 3\rho_0(\frac{\partial e_{\rm sym}(\rho)}{\partial\rho})|_{\rho=\rho_0}$, and the curvature parameter $K_{\rm sym} = 9\rho_0^2(\frac{\partial^2 e_{\rm sym}(\rho)}{\partial\rho^2})|_{\rho=\rho_0}$ and are obtained from the comparison of model calculations and experimental data, such as atomic masses [2–5], α-decay energies [6], nuclear charge radii [7], the thickness of the neutron skins of heavy nuclei [8,9], pygmy and giant dipole resonances [10–12], and nuclear isobaric analog-state energies [13]. Even though the deduced constraints are somewhat different in different studies, they are generally consistent with each other [14–17]. Examples are the values $S_0 = 31 \pm 2$ MeV and $L = 50 \pm 20$ MeV reported in Refs. [14,15] and the result of Ref. [17] providing a constraint centered around $(S_0, L) = (32.5, 70)$ MeV.

To probe the high-density behavior of the nuclear symmetry energy in terrestrial laboratories, we need the aid of HICs. Usually, the measured experimental data are compared with corresponding results of microscopic transport models in order to extract the information they carry with regard to properties of the symmetry energy. Several observables have been found or predicted to be sensitive to the nuclear symmetry energy such as, e.g., neutron and proton yields and flow ratios, double ratios, or differences, π^-/π^+ and K^0/K^+ meson production ratios, the Σ^-/Σ^+ ratio, and the balance energy of directed flow [18–32]. However, even though precise experimental data are available for some of these quantities, their interpretation is strongly model dependent and the obtained constraints on the nuclear symmetry energy at high densities are not consistent with each other (see, e.g., Refs. [14,15,17,33]).

Recently, the neutron-proton (or neutron-hydrogen) elliptic flow difference $v_2^n - v_2^{p,H}$ and ratio $v_2^n/v_2^{p,H}$ have been taken to constrain the high-density behavior of the nuclear symmetry energy. The elliptic flow parameter v_2 is the second-order coefficient in the Fourier expansion of the azimuthal distribution of detected particles

$$\frac{dN}{d\phi} = v_0[1 + 2v_1\cos(\phi) + 2v_2\cos(2\phi)] \quad (1)$$

and has the properties

$$v_2 \equiv \langle\cos(2\phi)\rangle = \frac{p_x^2 - p_y^2}{p_t^2}. \quad (2)$$

Here ϕ denotes the azimuthal angle of the considered outgoing particle with respect to the reaction plane and p_x and p_y are the

*liqf@hutc.zj.cn

two components of the transverse momentum $p_t = \sqrt{p_x^2 + p_y^2}$ in the so-oriented frame. The angular bracket denotes an average over all considered particles of a given event class. The parameter v_2 is thus a function of particle type, impact parameter, rapidity y, and transverse momentum p_t. By comparing calculations of two different versions of quantum molecular dynamics (QMD) models with the existing FOPI/LAND experimental data, a moderately soft to linear symmetry energy with a density dependence of its potential term proportional to $(\rho/\rho_0)^\gamma$ with the strength parameter $\gamma = 0.9 \pm 0.4$ (correspondingly, $L = 83 \pm 26$ MeV) and a moderately stiff to linear symmetry energy with the stiffness parameter $x = -1.35 \pm 1.0$ of the generalized Gogny force [34] (correspondingly, $L = 122 \pm 57$ MeV) have been reported in Refs. [23] and [25], respectively.

Furthermore, by using the newly updated ultrarelativistic quantum molecular dynamics (UrQMD) model in which the Skyrme potential energy density functional is introduced, the recently published flow data [35,36] of the FOPI Collaboration for light charged particles (protons, ^{2}H, ^{3}H, ^{3}He, and ^{4}He) can be reproduced quite well [37]. An advantage of the UrQMD update is that the stiffness of the symmetry energy can be more consistently selected within a broad range by simply changing Skyrme interactions, rather than by varying the exponent γ in the potential term of the symmetry energy, which, in addition, cannot be used to express a very soft symmetry energy [38]. It thus seems worthwhile to update the results of Ref. [23] within the framework of the newly updated UrQMD model, utilizing different Skyrme interactions with similar values of the isoscalar incompressibility but differing strengths of the symmetry energy.

In the work reported in Ref. [25], performed with a version of the Tübingen QMD model, the effects of uncertainties in several important ingredients of the transport model on the neutron-proton elliptic flow difference and ratio were carefully analyzed. They include, in addition to the symmetry energy, the incompressibility K_0 of nuclear matter, the nuclear optical potential, the in-medium nucleon-nucleon cross sections, and the momentum dependence of the symmetry potential. This work is important since most of these ingredients are still largely uncertain and their effects need to be assessed. In the current work an alternative strategy is pursued, consisting of first finding a set of model parameters which can "best" describe the FOPI flow data for charged light clusters, then exploring the sensitivity of the symmetry energy to the neutron-proton flow difference and ratio in various rapidity and transverse momentum intervals, and finally estimating the value of the slope parameter of the symmetry energy by comparing with the existing data. The overall model dependence can still be discussed during this process and will become apparent when comparing the calculations with the two members of the QMD family.

II. MODEL DESCRIPTION

The UrQMD model has been widely and successfully used to study nuclear reactions of $p+p$, $p+A$, and $A+A$ systems within a large range of beam energies, from SIS up to the LHC [39–42]. In the present code [37], the nuclear effective interaction potential energy U of the Hamiltonian H is derived from the integration of the Skyrme potential energy density functional, $U_\rho = \int u_\rho d^3\vec{r}$, and u_ρ reads

$$u_\rho = \frac{\alpha}{2}\frac{\rho^2}{\rho_0} + \frac{\beta}{\eta+1}\frac{\rho^{\eta+1}}{\rho_0^\eta} + \frac{g_{\rm sur}}{2\rho_0}(\nabla\rho)^2 + \frac{g_{\rm sur,iso}}{2\rho_0}[\nabla(\rho_n - \rho_p)]^2 + (A\rho^2 + B\rho^{\eta+1} + C\rho^{8/3})\delta^2 + g_{\rho\tau}\frac{\rho^{8/3}}{\rho_0^{5/3}}, \quad (3)$$

where α, β, η, $g_{\rm sur}$, $g_{\rm sur,iso}$, A, B,C, and $g_{\rho\tau}$ are parameters which can be directly calculated by using Skyrme parameters (see, e.g., Refs. [37,43]). It is known that the $\rho\tau$ term, obtained from the Thomas-Fermi approximation to the kinetic energy density, cannot fully represent the momentum dependence of the whole nonequilibrium dynamic process [43]. The momentum dependence of the real part of the optical potential (called "optical potential" for short in this paper) originating from that in Ref. [44] is also considered, as well as the Coulomb term. The importance of the optical potential for observables such as particle production and flow measured in HICs at intermediate energies has been widely investigated but its form is still far from being settled [44,45]. Recently, an isospin-dependent optical potential [34] was introduced into the isospin-dependent Boltzmann-Uehling-Uhlenbeck (IBUU04) transport model based on the Gogny effective interactions [46], giving rise to the issues of the momentum dependence of the symmetry energy and the associated neutron-proton effective mass splitting effect in the isospin asymmetric nuclear matter. Effects of the momentum-dependent symmetry potential or the neutron-proton effective mass splitting in HICs have been discussed recently [46–53]. But, it is still unclear whether the effective mass of neutrons is larger or smaller than that of protons in, for example, the neutron-rich nuclear medium [1,54–56]. While it is claimed that the neutron-proton elliptic flow difference is influenced to some extent by the momentum dependence of the nuclear symmetry potential in Refs. [49,52], it was reported in Ref. [53] that the flow difference does not exhibit a visible sensitivity to the momentum-dependent part of the isovector nucleon potential within the constraint of an asy-soft EoS, although the neutron-proton differential transverse flow does. Therefore, the influence of the neutron-proton effective mass splitting on observables in HICs certainly deserves further studies. However, together with support from previous QMD analyses, an isospin-independent form of the optical potential is still considered as appropriate for the current analysis of elliptic flows.

In this work, we choose 19 Skyrme interactions Skz4, BSk8, Skz2, BSk5, SkT6, SV-kap00, SV-mas08, SLy230a, SLy5, SV-mas07, SV-sym32, MSL0, SkO', Sefm081, SV-sym34, Rs, Sefm074, Ska35s25, and SkI1 [57], which give quite similar values of K_0 (within about 230 ± 10 MeV) but different L and $K_{\rm sym}$ values (the saturation properties of selected typical forces are shown in Table I). Moreover, in order to examine the influence of K_0 on the isospin-sensitive observables such as the elliptic flow ratio and difference, the parametrization sets SkA and SkI5 [57], giving larger incompressibility values than other sets, are also included. We notice from Table I and also from Ref. [57] that, due to the momentum dependence

TABLE I. Saturation properties of nuclear matter as obtained with selected Skyrme parametrizations used in this work.

	ρ_0 (fm^{-3})	E_0 (MeV)	K_0 (MeV)	S_0 (MeV)	L (MeV)	$K_{\rm sym}$ (MeV)	m^*/m
Skz4	0.160	−16.01	230.08	32.01	5.75	−240.86	0.70
Skz2	0.160	−16.01	230.07	32.01	16.81	−259.66	0.70
SV-mas08	0.160	−15.90	233.13	30.00	40.15	−172.38	0.80
MSL0	0.160	−16.00	230.00	30.00	60.00	−99.33	0.80
SkA	0.155	15.99	263.16	32.91	74.62	−78.46	0.61
SV-sym34	0.159	−15.97	234.07	34.00	80.95	−79.08	0.90
Ska35s25	0.158	−16.14	241.30	36.98	98.89	−23.57	0.99
SkI5	0.156	−15.85	255.79	36.64	129.33	159.57	0.58
SkI1	0.160	−15.95	242.75	37.53	161.05	234.67	0.69

of the Skyrme potential itself, values of the effective mass ratio m^*/m at normal density of selected sets still spread in a large range from about 0.6 up to 1.0 while the adopted optical potential provides an acceptable value of $m^*/m = 0.75$ at the Fermi momentum.

Figure 1 shows the density dependence of the symmetry energy for Skyrme interactions Skz2, SV-mas08, MSL0, SV-sym34, Ska35s25, and SkI1. In addition, the stiff (UrQMD-$\gamma = 1.5$) and soft (UrQMD-$\gamma = 0.5$) symmetry energies used in previous UrQMD calculations are shown for comparison and the symmetry energies deduced from the analyses of the FOPI π^-/π^+ ratios within the IBUU04 [21] and the Lanzhou quantum molecular dynamics (LQMD) [22] models are exhibited as well. It is apparent that the set of selected Skyrme forces covers the different forms of symmetry energies presented and currently discussed by theoretical groups.

The treatment of the collision term is the same as in our previous work [37] in which the FP4 parametrization of the in-medium nucleon-nucleon elastic cross section (NNECS) is adopted (except where stated otherwise). The program is stopped at 150 fm/c and then an isospin-dependent minimum

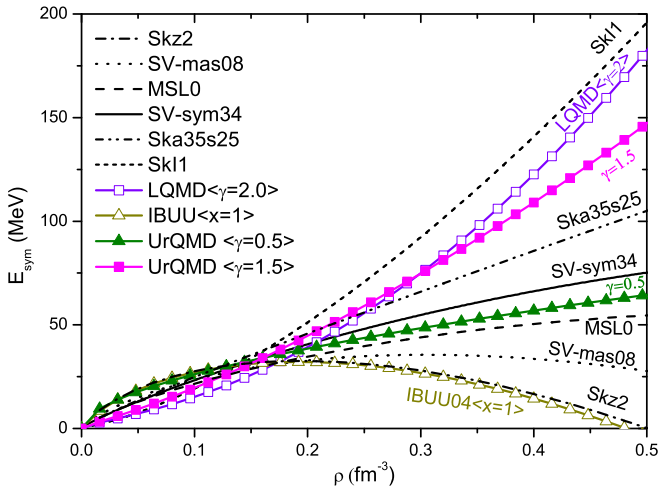

FIG. 1. (Color online) Density dependence of the symmetry energy for Skyrme interactions Skz2, SV-mas08, MSL0, SV-sym34, Ska35s25, and SkI1 (lines). Symmetry energies used in previous UrQMD [23] (lines with solid symbols), in LQMD [22] (line with open squares), and in IBUU04 [21] (line with open triangles) calculations are also shown for comparison.

span tree (iso-MST) algorithm is used to construct clusters. Nucleons with relative distances smaller than R_0 and relative momenta smaller than P_0 are considered to belong to the same cluster. In the present work, R_0 and P_0 are set to $R_0^{pp} = 2.8$ fm, $R_0^{nn} = R_0^{np} = 3.8$ fm, and $P_0 = 0.25$ GeV/c.

III. RESULTS AND DISCUSSIONS

As a first step, we try to describe the recent FOPI experimental data of the transverse momentum dependence of elliptic flow [36] using the updated UrQMD model. Figure 2 shows the u_{t0} dependence of the elliptic flow of protons and neutrons in semicentral ($0.25 < b_0 < 0.45$) ^{197}Au+^{197}Au collisions at $E_{\rm lab} = 400$ MeV/nucleon as calculated with the two parameter sets Skz4 and SkI1 for the two rapidity windows $|y_0| < 0.4$ and $0.4 < |y_0| < 0.6$. The reduced impact parameter b_0 is defined as $b_0 = b/b_{\rm max}$ with $b_{\rm max} = 1.15(A_P^{1/3} + A_T^{1/3})$. The scaled units $u_{t0} \equiv u_t/u_p$ and $y_0 \equiv y/y_p$ are used as done in Ref. [36]. The subscript p refers to the incident projectile in the center-of-mass system, and the subscript t denotes transverse (spatial) components. Here $u_t = \beta_t\gamma$ is the transverse component of the four-velocity $u = (\gamma, \beta\gamma)$ while the longitudinal rapidity is $y = 1/2\ln[(1+\beta_z)/(1-\beta_z)]$. The proton elliptic flow data for $|y_0| < 0.4$ [36] is shown with stars while calculations are given by the lines.

First, it is easily seen that the FOPI flow values of protons can be reproduced fairly well by both parameter sets in the whole u_{t0} region of the midrapidity window. The difference of K_0 obtained with Skz4 and SkI1 is only about 12 MeV while that of L is more than 150 MeV (Table I). This implies that elliptic flows of nucleons cannot be used individually to constrain the stiffness of the symmetry energy although they are known to be sensitive to the isoscalar part of the EoS. This is not unexpected as the contribution of the symmetry energy term is minor in comparison.

Second, if one compares the medium-modified NNECS adopted here (FU3FP4), following the results of Ref. [37], with the choice FU3FP1 suggested in Ref. [41], it is found that, in order to achieve the best description of the excitation function of collective flows, the medium corrections of NNECS should be gradually reduced with increasing beam energy. The restoration of the free NNECS should take place at lower relative momenta at the higher energies, a trend also reported in Ref. [43]. However, the need for an enhancement of the in-medium NNECS found there when describing the

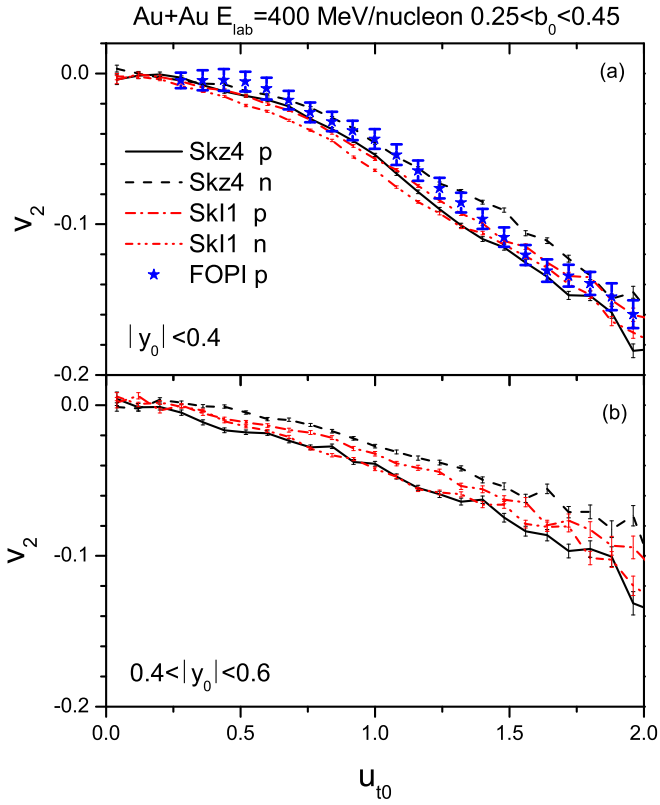

FIG. 2. (Color online) Elliptic flow v_2 of protons and neutrons in semicentral ($0.25 < b_0 < 0.45$) ^{197}Au+^{197}Au collisions at $E_{\rm lab} =$ 400 MeV/nucleon as a function of the normalized transverse component u_{t0} of the four-velocity. Calculations with Skz4 and SkI1 (lines) for the two rapidity windows $|y_0| < 0.4$ (a) and $0.4 < |y_0| < 0.6$ (b) are shown and, in the top panel, compared with the FOPI data for protons (stars) reported in Ref. [36].

elliptic flow of $Z \leqslant 2$ particles from midcentral ^{197}Au+^{197}Au collisions at about 400 MeV/nucleon is not evident here. From the current analysis, we find that this is likely due to the different particle species examined in the two studies. It is known that, mainly due to the lack of spin degrees of freedom in the QMD-like models, the yield of $Z = 2$ particles is largely underestimated. When taking the contribution of light clusters weighted by their numbers into account, irrespective of their mass numbers, the calculated absolute value of the elliptic flow for $Z \leqslant 2$ particles becomes slightly underestimated, an effect compensated with enhanced cross sections in the comparison with the experimental data for ^{197}Au+^{197}Au collisions reported in Ref. [43].

Finally, for both rapidity windows, we observe a small but opposite effect of Skz4 and SkI1 on proton and neutron elliptic flows. In the Skz4 case (soft symmetry energy), the squeeze-out of protons is much larger than that of neutrons, whereas in the SkI1 case (stiff symmetry energy), the trend is reversed: Neutrons show a larger squeeze-out than protons. The differences grow with increasing u_{t0}. As reported in Ref. [23], this phenomenon reflects the high density behavior of the symmetry energy.

In order to enlarge the symmetry energy effect and eliminate model-parameter dependences and other uncertainties of the individual flow observables, it is of interest to study the neutron-to-proton elliptic flow difference $v_2^n - v_2^p$ and ratio v_2^n/v_2^p [25,58]. In Fig. 3, calculations with Skz4, SV-sym34, and SkI1 for $v_2^n - v_2^p$ (upper two panels) and v_2^n/v_2^p (lower panels) are shown in two rapidity windows: $|y_0| < 0.4$ and $0.4 < |y_0| < 0.6$. The L value obtained with SV-sym34 is 80.95 MeV and lies between the two extremes obtained with Skz4 and SkI1 (Table I). Correspondingly, the flow differences and ratios calculated with this force are also centered in all plots. Furthermore, since the elliptic flows of neutrons and protons are negative within current conditions, the $v_2^n - v_2^p$ differences decrease while the v_2^n/v_2^p ratios increase with increasing L. With increasing u_{t0}, the sensitivity to the symmetry energy of $v_2^n - v_2^p$ (v_2^n/v_2^p) is enlarged (reduced), just because the absolute value of v_2 increases (Fig. 2). Finally, in both rapidity windows, but more so for $0.4 < |y_0| < 0.6$, the isospin effect on $v_2^n - v_2^p$ and v_2^n/v_2^p at about $0.5 < u_{t0} < 1.5$ is visibly large. Provided that the statistical errors will be small enough, intermediate rapidity windows may thus serve as promising kinematic regions in future experiments aiming at extracting a more precise information on the density dependence of the symmetry energy.

In the following, we recompare existing FOPI/LAND data, as reported in Ref. [23], with calculated elliptic flow ratios of neutrons vs protons or hydrogen isotopes. For better statistical accuracy in both calculations and experimental data, the elliptic flow ratio of neutrons vs hydrogen isotopes (v_2^n/v_2^H) is first considered as it is known to be equally sensitive to the symmetry energy, especially at smaller transverse momenta (cf. Fig. 3) where the experimental errors are relatively small. Figure 4 shows the comparison of the measured and the calculated ratios v_2^n/v_2^H as a function of the transverse momentum per nucleon p_t/A ($p_t/A = 0.431 u_{t0}$ GeV/c at $E_{\rm lab} = 400$ MeV/nucleon and A is the mass number of the emitted particles). SV-mas08&FP2 denote the result calculated with SV-mas08 and the FP2 parametrization of the NNECS [37,41]. All calculations were performed for the indicated impact parameter and rapidity intervals and gated with the range of laboratory angles accepted by LAND.

Similar to the results shown in Fig. 3, the v_2^n/v_2^H ratio increases with increasing L, from Skz4 to SkI5, and its spreading steadily grows when moving to the low transverse momentum region. When interpreting the results in more detail, it is seen that results calculated with SV-sym34 and SkA, for which the difference in L is only about 6 MeV, are almost overlapped even though the difference in K_0 is as large as almost 30 MeV and that of the effective mass ratio m^*/m is 0.3. It illustrates the sensitivity of the elliptic flow ratio to the stiffness of the symmetry energy and not to the incompressibility of the nuclear EoS. Also the big difference in m^*/m does not affect much the v_2^n/v_2^H ratio, which, at first glance, is not in agreement with previous work addressing the contribution of the momentum-dependent term to flow observables (see, e.g., Refs. [25,45]). However, as discussed for the $\rho\tau$ term in Eq. 3, the momentum-dependent contribution from the Skyrme potential energy density functional is very limited for the colliding conditions considered in the current work. The momentum dependence comes mainly from the optical potential which originates to

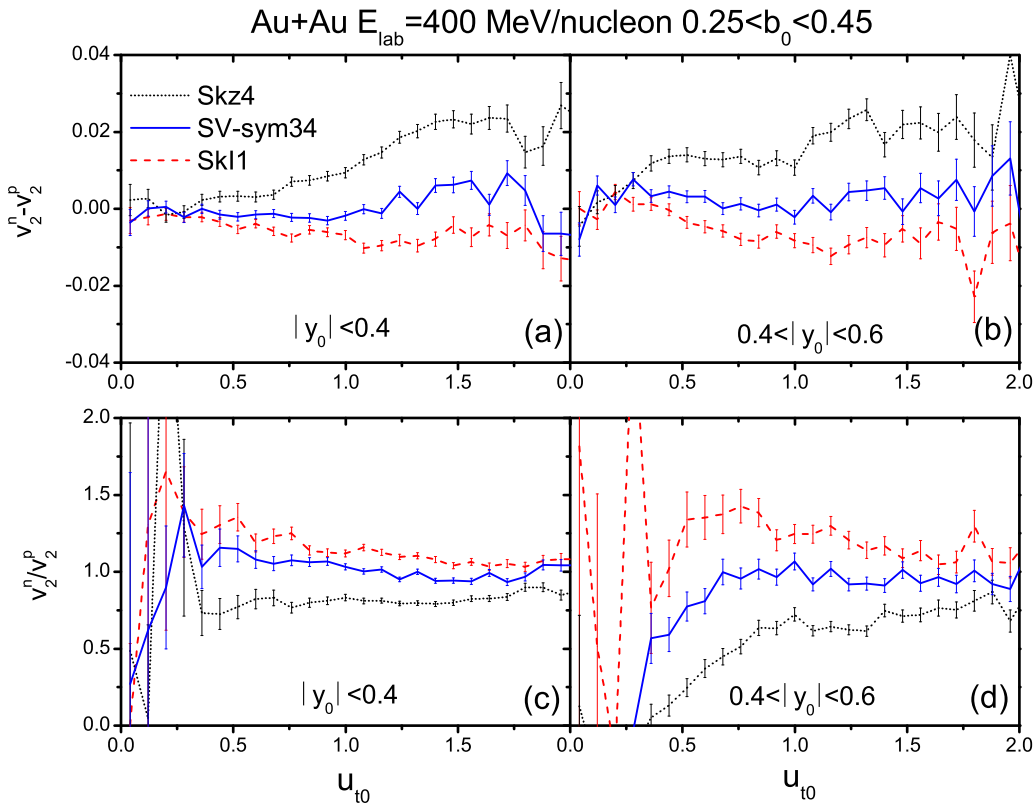

FIG. 3. (Color online) Dependence of the elliptic flow difference [panels (a) and (b)] and ratio [panels (c) and (d)] of free neutrons vs free protons produced in semicentral ^{197}Au+^{197}Au collisions at $E_{\rm lab} = 400$ MeV/nucleon as a function of the normalized transverse velocity u_{t0} for two rapidity windows $|y_0| < 0.4$ and $0.4 < |y_0| < 0.6$.

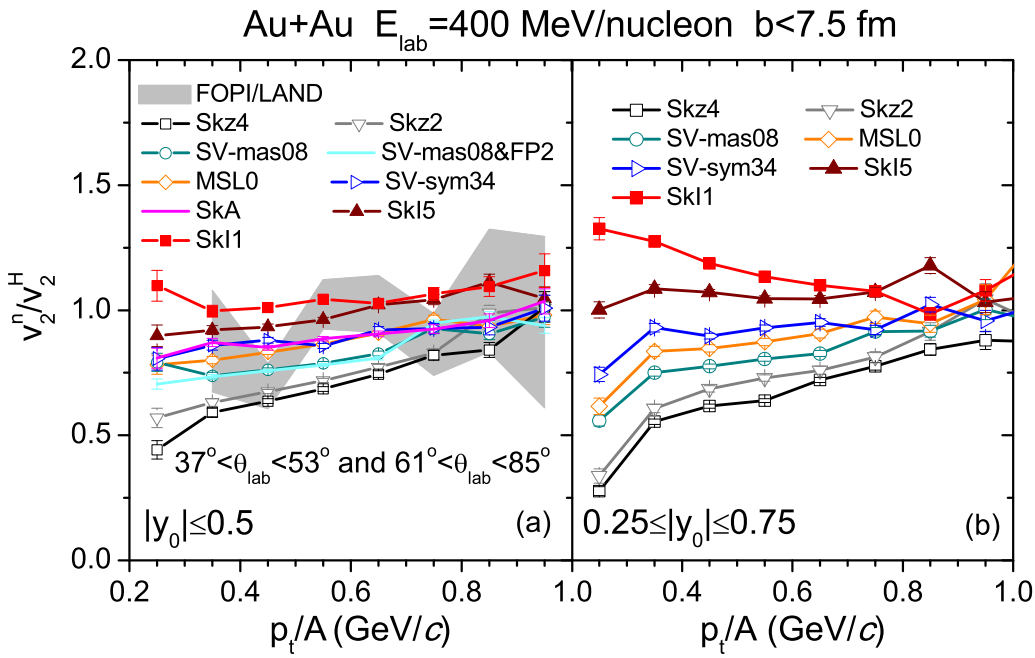

FIG. 4. (Color online) (a) Elliptic flow ratio of neutrons vs hydrogen isotopes ($Z = 1$) as a function of the transverse momentum p_t/A, calculated with the indicated nine Skyrme forces for central ($b < 7.5$ fm) ^{197}Au+^{197}Au collisions at $E_{\rm lab} = 400$ MeV/nucleon in the midrapidity interval $|y_0| \leqslant 0.5$ in comparison with the FOPI/LAND data (shaded area) reported in Ref. [23]; (b) the same quantity calculated with the indicated seven Skyrme forces for the intermediate rapidity interval $0.25 \leqslant |y_0| \leqslant 0.75$.

a large extent from a type of Lorentz force in a relativistic description. Actually, another parametrization of the optical potential suggested in Ref. [45] has also been tested and no visible effect on the elliptic flow ratio has been found, in line with the result of Ref. [53].

Furthermore, the results obtained with SV-mas08 & FP2 and SV-mas08 (i.e., with FP4) track each other closely, confirming the weak effect of the in-medium NNECS on the elliptic flow ratio already observed in Ref. [23]. Note that the isospin dependence in both the FP2 and FP4 NNECS parameterizations is not changed, which still represents an open question. Accordingly, the relative contributions of momentum- and density-modified NNECS to the flows of neutrons and hydrogen isotopes should not change much. A larger uncertainty assumed in the medium modifications of NNECS will definitely change the flow ratio visibly due to the change in the total collision numbers. In that case, however, the individual elliptic flows of neutrons and hydrogen isotopes will also vary largely, deviating from the experimental data shown in Fig. 2 and thus from our desired precondition. We may, therefore, conclude that the systematically increasing values of the elliptic flow ratio v_2^n/v_2^H calculated with the selected forces are mainly due to the increase of the stiffness of the symmetry energy and not to other changes of isoscalar components of the dynamic transport.

Figure 4(b) shows the calculation results for the intermediate rapidity window $0.25 \leqslant |y_0| \leqslant 0.75$, for the same impact parameter and rapidity interval but without the gate on laboratory angles. It is clearly seen that the differences of the various predictions steadily grow as one moves to the region of low transverse momentum. The v_2^n/v_2^H ratio in the rapidity window $0.25 \leqslant |y_0| \leqslant 0.75$ seems considerably more sensitive to the density-dependent symmetry energy than in the midrapidity interval $|y_0| \leqslant 0.5$, thus offering interesting opportunities for future experiments.

The results of fitting the transverse-momentum-dependent flow ratio [Fig. 4(a)] are shown in Fig. 5 as a function of the slope parameter L. The symbols represent the total χ^2 as calculated with the 21 Skyrme interactions. The variation with L is well described with a quadratic fit with an adjusted coefficient of determination (adj. R square) of 0.89. The obtained minimum of χ^2 corresponds to a slope parameter value $L = 89 \pm 45$ MeV within a 2-σ uncertainty. The so-obtained constraint is rather close to the $L = 83 \pm 52$ MeV (2-σ uncertainty) obtained previously [23]. The larger error in the latter case incorporates estimates of systematic deviations observed when studying the impact parameter dependence of the model comparisons. In fact, the fit result of $\gamma = 0.98 \pm 0.35$ obtained by Russotto *et al.* with the FP2 parametrization, corresponding to $L = 89 \pm 46$ MeV (2 σ), is identical to the value favored here, again supporting the sensitivity to the density dependence of the symmetry energy while details of the method are of reduced importance.

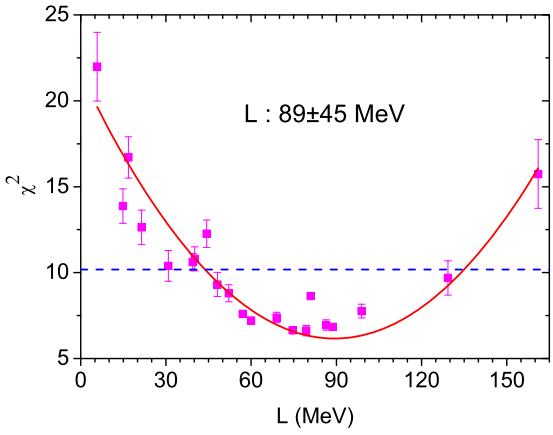

FIG. 5. (Color online) The total χ^2 characterizing the fit results obtained with the 21 studied Skyrme forces as a function of the slope parameter L. The smooth curve is a quadratic fit to the total χ^2, and the horizontal dashed line is used to determine the error of L within a 2-σ uncertainty.

It is interesting to see that the present result is slightly higher but still overlaps well with recent constraints for the symmetry energy at subnormal and normal densities, and even with constraints from astrophysical observations (see, e.g., Refs. [14–17,59]). Differences may arise to the extent that higher densities are probed with the present flow observables. We also note that a larger L reduces the difficulty of parameterizing the symmetry energy discussed by Dong *et al.* since $K_{\rm sym}$ is close to zero near the present central $L \approx 90$ MeV, according to the correlation established there [38]. Among the Skyrme forces in the favored L interval, we find the MSL0 parameter set ($L = 60$ MeV) which was based on a series of analyses of the neutron-skin thickness of heavy nuclei, isospin diffusion, and the double neutron/proton ratio in HICs at intermediate energies [9]. This force, as well as members of the families of SV-sym34 ($L = 81$ MeV) and Ska35s25 ($L = 99$ MeV), belong to the highly selected CSkP set of Skyrme forces favored by the analysis of Dutra *et al.* [57].

The quadratic behavior of χ^2 indicates that the flow ratio correlates linearly with L among the set of Skyrme forces studied. This is illustrated in Fig. 6 for the four observables $v_2^n - v_2^p$, $v_2^n - v_2^H$, v_2^n/v_2^p, and v_2^n/v_2^H. A linear fit describes the calculated correlation rather well in all cases. A comparison is made with the FOPI-LAND results obtained for these observables when sorted into the transverse-momentum interval 0.3 GeV/c$\leqslant p_t \leqslant$ 1.0 GeV/c. The selected intervals of L (with 1-σ uncertainty) largely overlap but also exhibit differences of up to about 25 MeV of their central values whose numerical average is close to $L = 85$ MeV. It will be interesting to see more precise data becoming available as, e.g., from the recent ASY-EOS (S394) experiment at GSI [60], which will be important also for testing the consistency of the model predictions.

As reported in Ref. [25], a slope parameter of $L = 122 \pm 57$ MeV was extracted with the help of the Tübingen QMD model. This is stiffer by about 30 MeV than the typical values that have been obtained here. As it turns out, this is only partly due to a possible model dependence because numerical uncertainties arise also from how the data are sorted. Cozma *et al.* start from an impact-parameter-dependent set of experimental values obtained by using the ratio ERAT of total transverse-to-longitudinal kinetic energies

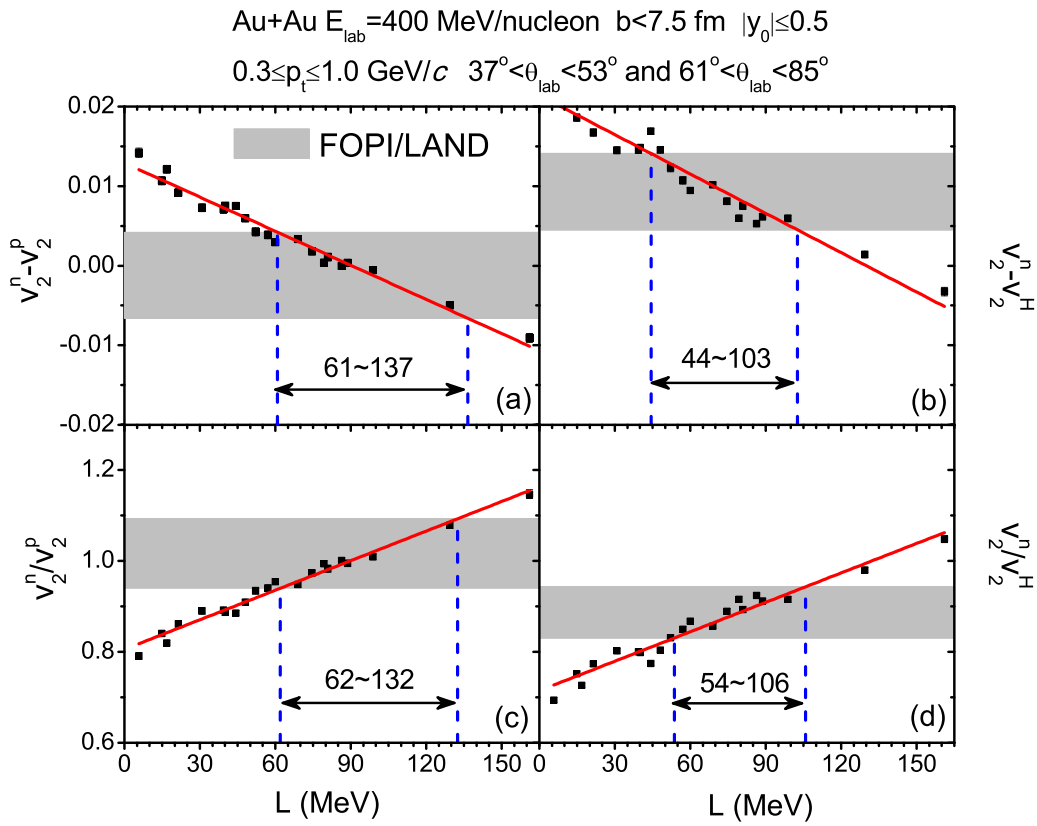

FIG. 6. (Color online) The elliptic flow differences $v_2^n - v_2^p$ (a) and $v_2^n - v_2^H$ (b) and the elliptic flow ratios v_2^n/v_2^p (c) and v_2^n/v_2^H (d) produced in moderately central ($b < 7.5$ fm) ^{197}Au+^{197}Au collisions at $E_{\rm lab} = 400$ MeV/nucleon are shown as a function of the slope parameter L. In each plot, the gray-shaded region indicates the p_t/A-integrated experimental data [23], full squares denote UrQMD calculations with the studied set of Skyrme forces, while the lines represent linear fits to the calculations.

in the center-of-mass system [36] for sorting according to centrality. Weighted averages were used to represent the impact-parameter-integrated ($b \leqslant 7.5$ fm) flow values. Even though the results are fully consistent within errors, they deviate slightly numerically from the multiplicity sorted values used by Russotto *et al.* as well as here. The numerical average deduced from comparing the neutron/proton and neutron/hydrogen differences and ratios with the calculations shown in Fig. 6 is near $L = 110$ MeV, reflecting a 25-MeV systematic uncertainty due to differences in impact-parameter sorting and in fitting correspondingly different azimuthal angular distributions. The remaining difference to $L = 122$ MeV may be ascribed to a residual model dependence of the UrQMD and Tübingen-QMD analyses. It is small in comparison to the quoted uncertainty $|\Delta L| = 57$ MeV which, to a large part, arises from unknown properties of the ingredients of transport models, including their isoscalar sector [25].

IV. SUMMARY AND OUTLOOK

To summarize, the recently released FOPI experimental data of the transverse-velocity dependence of elliptic flow of protons has been well described with the updated UrQMD transport model in which the Skyrme potential-energy-density functional is adopted for the mean-field part. The transverse-momentum-dependent elliptic flow ratios v_2^n/v_2^p and differences $v_2^n - v_2^p$ were shown to exhibit a larger sensitivity to the stiffness of the symmetry energy in the intermediate rapidity intervals $0.4 < |y_0| < 0.6$ than at midrapidity. As a function of the transverse velocity, the sensitivity of the flow ratios is enhanced at the lower and that of the differences at the higher transverse velocities. By comparing the calculations with the transverse-momentum-dependent FOPI/LAND flow ratio v_2^n/v_2^H the slope parameter of the density-dependent symmetry energy is extracted to be $L = 89 \pm 45$ MeV within a 2-σ confidence limit. Linear correlations of L with the predictions for ratios and differences for neutrons vs protons and neutrons vs all hydrogen isotopes have been established for the selected class of phenomenological forces. The results obtained from the comparison with the four transverse-momentum integrated experimental values are spread over an interval of $\Delta L \approx 25$ MeV but found to be consistent with each other within errors. Their numerical average is $L \approx 85$ MeV. A slightly larger slope parameter $L \approx 110$ MeV is obtained from a similar comparison with the flow data published in Ref. [25] for which the transverse-vs-longitudinal kinetic energy ratio ERAT has been used for the impact-parameter determination instead of the particle multiplicity used in Ref. [60]. More precise data will be needed to clarify to what extent these differences indicate residual systematic uncertainties or, possibly, mainly reflect the general statistical limits of the presently available experimental flow data.

The presented results are in full agreement with the previous studies performed with the UrQMD or Tübingen QMD models, indicating a moderately soft to linear density dependence of the symmetry energy. They contrast with diverging results obtained from the comparisons of IBUU or LQMD model calculations with the FOPI π^-/π^+ ratios from which both extremely soft and extremely stiff behaviors were extracted. The obtained slope parameter of $L \approx 90$–110 MeV is larger than the typical $L = 60$ MeV resulting from nuclear structure studies and reactions at lower energies. If confirmed with more precise data, this may reflect the higher densities probed at the present energy as well as the approximations made with parametrizations and extrapolations. It is clear that new experiments addressing the strength and density dependence of the symmetry energy, as presently performed or in preparation at several laboratories, will play an important role in clarifying these questions.

On the theoretical side, the nonequilibrium effect is one of the most important characteristics of heavy-ion collisions at intermediate energies for which the isospin degree of freedom can be used as a sensitive probe. The issue of the degree of isospin equilibrium should receive more attention, including the investigation of the isospin dependence in both the momentum-modified mean-field potentials and the binary scatterings representing the in-medium nuclear interaction. In a future study, this problem will be addressed within the same microscopic transport model.

ACKNOWLEDGMENTS

The authors thank W. Reisdorf for providing experimental data and acknowledge support by the computing server C3S2 in Huzhou Teachers College and the warm hospitality of the Frankfurt Institute for Advanced Studies (FIAS), Johann Wolfgang Goethe-Universität, Germany. The work is supported in part by the National Natural Science Foundation of China (Grants No. 11175074 and No. 11375062), the Qian-Jiang Talents Project of Zhejiang Province (Grant No. 2010R10102), and the project sponsored by SRF for ROCS, SEM.

[1] B. A. Li, L. W. Chen, and C. M. Ko, Phys. Rep. **464**, 113 (2008).
[2] B. K. Agrawal, J. N. De, S. K. Samaddar, G. Colo, and A. Sulaksono, Phys. Rev. C **87**, 051306 (2013).
[3] M. Liu, N. Wang, Z. X. Li, and F. S. Zhang, Phys. Rev. C **82**, 064306 (2010).
[4] P. Möller, W. D. Myers, H. Sagawa, and S. Yoshida, Phys. Rev. Lett. **108**, 052501 (2012).
[5] L. W. Chen, Phys. Rev. C **83**, 044308 (2011).
[6] J. Dong, W. Zuo, and J. Gu, Phys. Rev. C **87**, 014303 (2013).
[7] N. Wang and T. Li, Phys. Rev. C **88**, 011301 (2013).
[8] M. Centelles, X. Roca-Maza, X. Viñas, and M. Warda, Phys. Rev. Lett. **102**, 122502 (2009); M. Warda, X. Viñas, X. Roca-Maza, and M. Centelles, Phys. Rev. C **81**, 054309 (2010).
[9] L. W. Chen, C. M. Ko, B. A. Li, and J. Xu, Phys. Rev. C **82**, 024321 (2010).
[10] A. Carbone, G. Colo, A. Bracco, L. G. Cao, P. F. Bortignon, F. Camera, and O. Wieland, Phys. Rev. C **81**, 041301 (2010).
[11] L. Trippa, G. Colo, and E. Vigezzi, Phys. Rev. C **77**, 061304 (2008).
[12] X. Roca-Maza, M. Brenna, B. K. Agrawal, P. F. Bortignon, G. Colo, L.-G. Cao, N. Paar, and D. Vretenar, Phys. Rev. C **87**, 034301 (2013).
[13] P. Danielewicz and J. Lee, Nucl. Phys. A **818**, 36 (2009).
[14] B. A. Li, L. W. Chen, F. J. Fattoyev, W. G. Newton, and C. Xu, J. Phys. Conf. Ser. **413**, 012021 (2013).
[15] L.-W. Chen, arXiv:1212.0284 [nucl-th].
[16] J. M. Lattimer and Y. Lim, ApJ **771**, 51 (2013).
[17] M. B. Tsang, J. R. Stone, F. Camera, P. Danielewicz, S. Gandolfi, K. Hebeler, C. J. Horowitz, J. Lee *et al.*, Phys. Rev. C **86**, 015803 (2012).
[18] M. Di Toro, V. Baran, M. Colonna, and V. Greco, J. Phys. G **37**, 083101 (2010).
[19] M. B. Tsang, Y. Zhang, P. Danielewicz, M. Famiano, Z. Li, W. G. Lynch, and A. W. Steiner, Phys. Rev. Lett. **102**, 122701 (2009); M. B. Tsang *et al.*, Int. J. Mod. Phys. E **19**, 1631 (2010).
[20] X. Lopez, Y. J. Kim, N. Herrmann, A. Andronic, V. Barret, Z. Basrak, N. Bastid, M. L. Benabderrahmane *et al.*, Phys. Rev. C **75**, 011901 (2007).
[21] Z. Xiao, B. A. Li, L. W. Chen, G. C. Yong, and M. Zhang, Phys. Rev. Lett. **102**, 062502 (2009).
[22] Z. Q. Feng and G. M. Jin, Phys. Lett. B **683**, 140 (2010).
[23] P. Russotto, P. Z. Wu, M. Zoric, M. Chartier, Y. Leifels, R. C. Lemmon, Q. Li, J. Łukasik *et al.*, Phys. Lett. B **697**, 471 (2011).
[24] M. D. Cozma, Phys. Lett. B **700**, 139 (2011).
[25] M. D. Cozma, Y. Leifels, W. Trautmann, Q. Li, and P. Russotto, Phys. Rev. C **88**, 044912 (2013).
[26] S. Kumar, Y. G. Ma, G. Q. Zhang, and C. L. Zhou, Phys. Rev. C **85**, 024620 (2012).
[27] W. J. Xie, J. Su, L. Zhu, and F. S. Zhang, Phys. Lett. B **718**, 1510 (2013).
[28] Q. Li, Z. Li, S. Soff, R. K. Gupta, M. Bleicher, and H. Stöcker, J. Phys. G **31**, 1359 (2005).
[29] Q. Li, Z. Li, E. Zhao, and R. K. Gupta, Phys. Rev. C **71**, 054907 (2005).
[30] S. Gautam, A. D. Sood, K. Uri, and J. Aichelin, Phys. Rev. C **83**, 014603 (2011).
[31] Y. Wang, C. Guo, Q. Li, and H. Zhang, Sci. China Phys. Mech. Astron. **55**, 2407 (2012).
[32] C. Guo, Y. Wang, Q. Li, W. Trautmann, L. Liu, and L. Wu, Sci. China Phys. Mech. Astron. **55**, 252 (2012).
[33] H. Wolter, *Proceedings of the 50th International Winter Meeting on Nuclear Physics, Bormio, Italy, 23–27 January 2012*.
[34] C. B. Das, S. Das Gupta, C. Gale, and A.-A. Li, Phys. Rev. C **67**, 034611 (2003).
[35] W. Reisdorf *et al.* (FOPI Collaboration), Nucl. Phys. A **848**, 366 (2010).
[36] W. Reisdorf *et al.* (FOPI Collaboration), Nucl. Phys. A **876**, 1 (2012).
[37] Y. Wang, C. Guo, Q. Li, H. Zhang, Z. Li, and W. Trautmann, Phys. Rev. C **89**, 034606 (2014).

[38] J. Dong, W. Zuo, J. Gu, and U. Lombardo, Phys. Rev. C **85**, 034308 (2012).
[39] S. A. Bass *et al*. (UrQMD Collaboration), Prog. Part. Nucl. Phys. **41**, 255 (1998).
[40] M. Bleicher, E. Zabrodin, C. Spieles, S. A. Bass, C. Ernst, S. Soff, L. Bravina, M. Belkacem *et al*., J. Phys. G **25**, 1859 (1999).
[41] Q. Li, C. Shen, C. Guo, Y. Wang, Z. Li, J. Łukasik, and W. Trautmann, Phys. Rev. C **83**, 044617 (2011).
[42] Q. Li, G. Graf, and M. Bleicher, Phys. Rev. C **85**, 034908 (2012).
[43] Y. Zhang and Z. Li, Phys. Rev. C **74**, 014602 (2006).
[44] J. Aichelin, A. Rosenhauer, G. Peilert, H. Stoecker, and W. Greiner, Phys. Rev. Lett. **58**, 1926 (1987).
[45] C. Hartnack and J. Aichelin, Phys. Rev. C **49**, 2801 (1994).
[46] B.-A. Li, C. B. Das, S. Das Gupta, and C. Gale, Phys. Rev. C **69**, 011603 (2004).
[47] L.-W. Chen, C. M. Ko, and B.-A. Li, Phys. Rev. C **69**, 054606 (2004); Phys. Rev. Lett. **94**, 032701 (2005).
[48] V. Baran, M. Colonna, V. Greco, and M. Di Toro, Phys. Rep. **410**, 335 (2005).
[49] V. Giordano, M. Colonna, M. Di Toro, V. Greco, and J. Rizzo, Phys. Rev. C **81**, 044611 (2010).
[50] Y. Gao, L. Zhang, H.-F. Zhang, X.-M. Chen, and G.-C. Yong, Phys. Rev. C **83**, 047602 (2011).
[51] Z.-Q. Feng, Phys. Rev. C **84**, 024610 (2011); Phys. Lett. B **707**, 83 (2012).
[52] Z.-Q. Feng, Nucl. Phys. A **878**, 3 (2012).
[53] L. Zhang, Y. Gao, Y. Du, G.-H. Zuo, and G.-C. Yong, Eur. Phys. J. A **48**, 30 (2012).
[54] M. Di Toro, M. Colonna, and J. Rizzo, AIP Conf. Proc. **791**, 70 (2005).
[55] E. N. E. van Dalen, C. Fuchs, and A. Faessler, Phys. Rev. Lett. **95**, 022302 (2005); Phys. Rev. C **72**, 065803 (2005).
[56] Y. Zhang, M. B. Tsang, Z. Li, and H. Liu, arXiv:1402.3790 [nucl-th].
[57] M. Dutra, O. Lourenco, J. S. Sa Martins, A. Delfino, J. R. Stone, and P. D. Stevenson, Phys. Rev. C **85**, 035201 (2012); M. Dutra, Ph.D. thesis, Universidade Federal Fluminense, 2011.
[58] W.-M. Guo, G.-C. Yong, Y. Wang, Q. Li, H. Zhang, and W. Zuo, Phys. Lett. B **726**, 211 (2013).
[59] A. W. Steiner, J. M. Lattimer, and E. F. Brown, Astrophys. J. Lett. **765**, L5 (2013).
[60] P. Russotto *et al*. (ASY-EOS Collaboration), J. Phys. Conf. Ser. **420**, 012092 (2013).